

**Infection of Epstein-Barr virus in periapical granulomas and
its reactivation by butyric acid from
*Porphyromonas endodontalis***

Kosuke Makino

**Nihon University Graduate School of Dentistry,
Major in Endodontics**

(Directors: Prof. Bunnai Ogiso and Assoc. Prof. Osamu Takeichi)

Abstract

Periapical periodontitis is caused by polymicrobial infection. Treatment with antibacterial agents is normally performed to eliminate bacteria from root canals; however, tooth extraction is often selected if root canal treatment does not work well. Therefore, bacteria and other microorganisms could be involved in this disease. Recently, Epstein-Barr virus (EBV) was detected in periapical periodontitis lesions; however, evidence for EBV infection has not been fully examined. EBV stays in latency after infection, and is reactivated by *n*-butyric acid, which is a metabolic product from some bacterial species. This suggests that latent EBV could be reactivated by association with the bacteria in periapical lesions. To elucidate the role of EBV on the pathogenesis of the periapical lesions, periapical granulomas were examined for EBV and *Porphyromonas endodontalis* (one of periapical periodontopathic bacteria). Surgically-removed periapical lesions were obtained and divided into two portions. One was prepared as paraffin sections and pathologically-examined using hematoxylin-eosin stains. Only 50 of 63 lesions were periapical granulomas and were examined further. The other portion was used for DNA extraction to detect EBV and *P. endodontalis* using real-time PCR. EBV DNA was detected in 38 of 50 periapical granulomas (76.0%), and the median number of EBV DNA copies was approximately 6,634.00 / μ g total DNA; whereas, EBV

DNA was not detected in healthy gingival tissues (n = 10). *P. endodontalis* was detected in 32 of 50 periapical granulomas (64.0%) and in 5 of 10 healthy gingival tissues (50%). Paraffin sections were also analyzed by *in situ* hybridization to detect EBV-encoded small RNA (EBER)-expressing cells. EBER was detected in the cytoplasm and nuclei of B lymphocytes and plasma cells in six of nine periapical granulomas, but not in healthy gingival tissues. In addition, immunohistochemical analysis for latent membrane protein 1 (LMP-1) of EBV using serial tissue sections showed that LMP-1-expressing cells were localized to the same areas as EBER-expressing cells. The culture supernatant of *P. endodontalis* was quantified using ion-exclusion high-performance liquid chromatography and the concentration of *n*-butyric acid was 23.38 ± 3.67 mM (n = 5). Daudi cell line was then treated with commercially available *n*-butyric acid or culture supernatants of *P. endodontalis* and the expression of immediate early gene BZLF1 mRNA, known as the marker of EBV reactivation was detected in a time-dependent manner in the culture supernatant. These data suggested the possibility that B lymphocytes and plasma cells in periapical granulomas are the major source of EBV infection and latent EBV could be reactivated by *P. endodontalis* in periapical granulomas. These findings are consistent with a hypothesis suggesting that reactivated EBV could play a pivotal role in controlling immune cell responses in periapical

granulomas.

This article was prepared using the original article “Epstein-Barr Virus Infection in Chronically Inflamed Periapical Granulomas” (Kosuke Makino, Osamu Takeichi, Keisuke Hatori, Kenichi Imai, Kuniyasu Ochiai, Bunnai Ogiso, PLoS ONE 10(4), e0121548, 2015) with the additional data on EBV reactivation in periapical granulomas.

Introduction

Periapical periodontitis is characterized by supporting tissue damage and progressive alveolar bone resorption around the apical areas of affected teeth (1). It is caused by a mixed bacterial infection in the oral cavity, and dental caries is thought to be a major source of this infection (2). Periodontopathic bacteria such as *Porphyromonas gingivalis*, *Fusobacterium nucleatum*, and *Eubacterium* species are microbiological research foci in dentistry because they produce lipopolysaccharide (LPS), a strong virulence factor (3). A local drug delivery system using a combination of three antibiotics (minocycline, ciprofloxacin, and metronidazole) has been reported to eliminate periodontopathic bacteria through root canals and to be effective for the treatment of patients with periapical periodontitis (4). Nevertheless, some patients are not healed following the application of antibiotics; such cases of chronic inflammation are referred to as persistent

periapical periodontitis (5), suggesting that antibacterial drug-resistant microorganisms such as viruses or fungi could be present in the periapical lesions. Unfortunately, tooth extraction is often planned for the treatment of these patients. Thus, more effective pharmacological therapies must be developed to preserve teeth.

Epstein-Barr virus (EBV) is an oncogenic herpesvirus that infects a significant percentage (> 90%) of the population worldwide and is the causative agent of infectious mononucleosis (6). It is detected frequently in Burkitt's lymphoma, Hodgkin's disease, and T-cell lymphoma. Thus, EBV has been implicated in the pathogenesis of several malignancies. EBV infection induces the expression of proinflammatory cytokines, such as tumor necrosis factor (TNF)- α , interleukin (IL)-1 β , IL-8, IL-10, IL-12 and IL-17 (7-9). Therefore, EBV could be associated with both carcinogenesis and pathogenesis in local inflammation.

A correlation between EBV infection and rheumatoid arthritis (10) and Sjögren syndrome (11) has also been shown. These observations suggest that EBV infection in periapical periodontitis could be related to tissue injury and cell damage.

Recently, the presence of EBV in periapical lesions has been examined by immunohistochemistry for EBV nuclear antigen (EBNA) or PCR (12-14); however, direct evidence of EBV infection in periapical lesions has not been examined yet. *In situ*

hybridization (ISH) for EBV-encoded small RNA (EBER) and immunohistochemistry for latent membrane protein 1 (LMP-1) of EBV were performed to identify EBV infection. EBER is expressed in latent EBV-infected cells and can be used as a target for the detection of EBV-infected cells in tissues (15).

EBV shows latency after infection. During latent EBV infection, immediate early gene BZLF-1 is expressed with substantial stimuli (16). BZLF-1 is a regulator for productive replication of EBV. Thus, the expression of BZLF-1 mRNA plays a pivotal role in controlling EBV replication and is most likely associated with the pathosis of periapical periodontitis.

It has been shown that BZLF-1 is expressed by EBV-infected B-lymphocytes in the presence of *n*-butyric acid (17). Butyric acid is a saturated, short chain fatty acid (SCFA) with a 4-carbon acid and has a structural isomer called iso-butyric acid. Butyric acid is produced through fermentation by obligate anaerobic bacteria; therefore, periapical lesions might be a reservoir of *n*-butyric acid, suggesting that BZLF-1 expression could be upregulated by the association with *n*-butyric acid in periapical lesions.

Porphyromonas endodontalis is a black-pigmented, gram-negative anaerobe related to endodontic infections and pulp necrosis (18). The colonization of *P. endodontalis* causes periapical lesions with acute symptoms, such as pain and swelling in response to

purulent inflammation (19). Similarly, *P. endodontalis* induces inflammatory cytokines with stimulation by LPS (20), and causes subsequent bone resorption (21). Therefore, *P. endodontalis* is important in mediating periapical pathosis and, more importantly, could be a major target.

This study examined the evidence of EBV infection in periapical granulomas, and whether latent EBV is reactivated by *P. endodontalis*.

Materials and Methods

Patients

In total, 63 patients (22 males and 41 females; age range 24-78 years), who were referred to the Department of Endodontics at Nihon University School of Dentistry Dental Hospital (Tokyo) because of persistent periapical periodontitis were included in this study. The clinical symptoms of the patients included an absence of throbbing pain, pain on palpation of the mucosa around the root apex, and percussion pain. An apparent radiolucency was seen around the root apex of all teeth (Fig. 1A). Endodontic treatments had been applied several times by general practitioners; however, the patients were still experiencing symptoms. Therefore, endodontic surgery (apicoectomy and retrograde filling) was selected. Patients had no systemic diseases, and antibiotics have

not been taken during the previous 6 months. This study was approved by the ethics committee of Nihon University School of Dentistry, based on the Declaration of Helsinki. Before sample collection, the experimental design, risks, and potential for discomfort were explained fully, and all patients signed consent forms. Healthy gingival tissues were obtained at the time of extraction of impacted wisdom teeth from 10 patients (5 males and 5 females; age range 15-41 years), who were referred to the Department of Oral Surgery. These patients had no clinical symptoms, such as pain or swelling, and an X-ray examination did not indicate inflammation.

Pathological Examination of the Samples

The periapical lesions (Fig. 1B) and healthy gingival tissues, which were removed from the patients at the time of surgical treatment, measured approximately 0.82 and 0.44 cm in diameter, respectively. The tissues were fixed immediately in acetone and then embedded in paraffin. Serial tissue sections (7 μm in thickness) were prepared. A pathological examination of the specimens was performed after hematoxylin and eosin staining. Sectioned areas were selected randomly, and at least three different regions in each sample were examined. The sections were investigated using a light microscope (Olympus BH-2, Tokyo, Japan). Periapical granulomas and healthy gingival tissues,

which were confirmed pathologically, were utilized for the following studies.

Quantitative Analysis of the EBV DNA Copy Number

EBV in the periapical granuloma and healthy gingival tissue samples was detected quantitatively using real-time PCR. In brief, DNA was extracted from paraffin sections of periapical granulomas or healthy gingival tissues using a QIAamp DNA Mini Kit (Qiagen, Hilden, Germany). In total, 40 ng of each DNA sample was amplified in a 25- μ l reaction mixture containing SYBR Premix Ex Taq (Takara Bio Inc., Shiga, Japan) and 20 μ M each of the sense and antisense PCR primers for EBV. The sequences of the primers were: 5'-TGCTTCGTTATAGCCGTAGT-3' (reverse) and: 5'-CCTGGTCATCCTTTG CCA-3' (forward). Amplification was conducted in 40 cycles of 95°C for 15 s and 60°C for 60 s using a Smart Cycler (Cepheid, CA, USA). For the preparation of a standard curve to determine the EBV DNA copy number, a 10-fold serial dilution of a known quantity of EBV DNA (approximately 1×10^6 copies/ μ l) was prepared. Each diluted DNA sample was amplified using real-time PCR alongside the DNA extracted from the specimens. A standard curve was prepared using semi-log graphs, and the EBV DNA copy number in the specimens was calculated.

ISH to Detect EBER-Expressing Cells

ISH using EBER-specific probes was employed. Periapical granulomas (n = 9), contained more than 6,650 EBV DNA copies, which were determined using quantitative real-time PCR, were examined. In brief, deparaffinized sections were digested with proteinase K for 30 min and then hybridized with hapten 5-carboxy-fluorescein-labeled 15-nucleotide single-stranded DNA probes for EBV (Dako, Glostrup, Denmark) at 55°C for 90 min. After a stringent wash with 0.5× SSC, horseradish peroxidase-conjugated anti-FITC rabbit polyclonal antibodies (Dako) were incubated with the mixture for 30 min. Finally, a colorimetric reaction using 3,3'-diaminobenzidine (DAB; Vector Laboratories, CA, USA) was performed, followed by counterstaining with hematoxylin. EBER expression in periapical granulomas was compared with healthy gingival tissues (n = 5). Tissue sections of human malignant lymphomas were used as a positive control for EBER ISH. The negative control constituted hybridization without the addition of the EBER probe.

Immunohistochemical Analysis

To examine the localization of LMP-1-expressing cells, periapical granulomas (n = 6) confirmed for EBER mRNA expression by ISH and healthy gingival tissues (n = 5) were

investigated. Serial paraffin sections of EBER-positive specimens were analyzed. In brief, the paraffin sections were deparaffinized, rehydrated, and incubated with 0.3% H₂O₂ in methanol for 30 min to quench endogenous peroxidase. The sections were incubated first with 10% normal horse serum (Vector Laboratories) to block non-specific binding for 20 min, followed by human LMP-1 monoclonal antibodies (1:100 in PBS; Dako), followed by biotinylated anti-mouse IgG antibodies (Vector Laboratories), and finally with avidin-biotin peroxidase complex. To reveal LMP-1-positive cells via color development, the horseradish peroxidase substrate (DAB) was used, and hematoxylin counterstaining was performed. Normal mouse IgG antibodies (Cayman Chemical, MI, USA) were used as a negative control in place of anti-LMP-1 antibodies.

Bacterial Strain and Culture Conditions

P. endodontalis (JCM8526) was purchased from Japan Collection of Microorganisms (RIKEN BRC, Ibaraki, Japan). *P. endodontalis* was cultured in Gifu Anaerobic Medium (GAM) broth (Nissui, Tokyo, Japan) with hemin (5.0 ppm) and menadione (0.5 ppm) for 5 days at 37°C in anaerobic conditions (5% CO₂, 10% H₂ and 85% N₂, Model 1024, Forma Scientific, Marietta, OH)

Quantitative Detection of *P. endodontalis* using Real-time PCR

P. endodontalis was detected quantitatively using real-time PCR. The same DNA samples as in the detection study of EBV DNA (periapical granulomas and healthy gingival tissues) were used. The following PCR primers were used:

5'-GCTGCAGCTCAACTGTAGTCTTG-3' (forward),

5'-TCAGTGTCAGACGGAGCCTAGTAC-3' (reverse). PCR amplification was performed with SYBR Premix Ex Taq in 40 cycles of 95°C for 15 s and 60°C for 60 s using Smart Cycler. To set up the standard curve, a 10-fold serial dilution of a known quantity of *P. endodontalis* gene (approximately 1×10^8 cells/ml) was prepared. Each diluted DNA sample was amplified using real-time PCR alongside the DNA extracted from the specimens. A standard curve was prepared using semi-log graphs and the number of *P. endodontalis* in the specimens was calculated.

Quantitative Analysis of *n*-Butyric Acid in *P. endodontalis* Culture Supernatants

The culture supernatant of *P. endodontalis* was collected and *n*-butyric acid was quantified using ion-exclusion high-performance liquid chromatography (HPLC), as described previously (22). In brief, the supernatant was mixed with 12% perchloric acid and was filtered using cellulose acetate membrane filter (CosmoniceFilter W, pore size; 0.45 μ m, Nacalai tesque, Kyoto, Japan). The supernatant was injected into SIL-10

autoinjector (Shimadzu, Kyoto, Japan). *n*-Butyric acid was separated using a serial organic acid column with a guard column with isocratic elution of *p*-toluene sulfonic acid aqueous solution and was detected with an electronic conductivity detector.

Detection of BZLF-1 mRNA Expression using Real-time PCR

Daudi cell line (EBV-positive human B lymphoblastoid cell line) was cultured using RPMI-1640 culture medium (Sigma, MO, USA) with 10% FBS and 1% penicillin-streptomycin at 37°C. The cells (2×10^6 cells/well) were seeded into a 12-well culture plates. After 4 h, the cells were treated with *n*-butyric acid (Wako, Osaka, Japan; 1.0 mM) for 48 h or the supernatants of *P. endodontalis* (1.2 mM) for 3, 6, 12, and 24 h. Total RNA was extracted using RNeasy Mini Kit (Qiagen), according to the manufacturer's instructions, followed by treatment with QIA shredder (Qiagen). RNA was reverse-transcribed using PrimeScript RT reagent kit (Takara Bio Inc.) and the complimentary DNA was amplified by real-time PCR using SYBR Premix Ex Taq. The sequence of PCR primers was as follows:

BZLF-1 forward, 5'-CCATACCAGGTGCCTTTTGT-3';

BZLF-1 reverse, 5'-GAGACTGGGAACAGCTGAGG-3';

GAPDH forward, 5'-GCACCGTCAAGGCTGAGAAC-3';

GAPDH reverse, 5'-ATGGTGGTGAAGACGCCAGT-3'.

The amplification protocol of BZLF-1 and GAPDH was 40 cycles of 95°C for 5 s, 60°C for 20 s and 30 cycles of 95°C for 5 s, 60°C for 20 s, respectively. After amplification, BZLF-1 message was divided by the message of GAPDH to normalize PCR amplification.

Statistical Analysis

Statistical analysis was performed using SPSS version 15.0 for Windows (SPSS, IL, USA). The comparison of EBV detection between periapical granulomas and healthy gingival tissues was made using a Mann-Whitney *U*-test. Experiments using Daudi cell line were statistically analyzed using Student's *t*-test and Dunnett's test. A statistical difference was considered at $p < 0.05$.

Results

Pathological Examination of the Samples

Surgically-removed periapical lesions were examined pathologically. Among the 63 periapical lesions stained with hematoxylin and eosin, 50 exhibited granulomatous tissues with large numbers of microvessels and inflammatory cells such as

polymorphonuclear leukocytes (PMNs), lymphocytes, plasma cells, and macrophages (Fig. 2A). No epithelial cells were observed, and the specimens were diagnosed as periapical granulomas. The remaining periapical lesions exhibited an epithelial cell lining with cholesterol clefts in granulomatous tissue and were diagnosed as radicular cysts (Fig. 2B); these were not used in this study. The healthy gingival tissues contained more collagen fibers and fewer inflammatory cells in the granulomatous tissue than periapical granulomas (Fig. 2C).

Quantitative Analysis of EBV DNA Copy Numbers

DNA extracted from periapical granulomas and healthy gingival tissues was amplified using real-time PCR with EBV-specific primers. A standard curve was prepared after PCR amplification using serially diluted EBV DNA (as shown in Fig. 3A) and PCR was performed at the same time as the amplification of DNA from periapical granulomas and healthy gingival tissues. Among the 50 periapical granulomas, 38 specimens (76.0%) exhibited the presence of EBV (Table 1). The median EBV DNA copy number was approximately 6,634.00 / μ g total DNA (Fig. 3B). In contrast, EBV DNA was not detected in the healthy gingival tissues. A statistical analysis demonstrated that the EBV detection rate in periapical granulomas was significantly higher than that in healthy

gingival tissues ($p = 0.0001$).

ISH for EBER and Immunohistochemistry for LMP-1

In situ detection using EBER-specific probes was performed for periapical granulomas and healthy gingival tissues. In total, six of nine periapical granulomas (66.7%) showed positive expression of EBER (Fig. 4A-F). EBER localization was exhibited in the nucleus and cytoplasm of B lymphocytes and plasma cells. In contrast, EBV-negative periapical granulomas (Fig. 4G-I) and healthy gingival tissues (Fig. 4J) did not show EBER positivity. No expression was detected using a sense probe for EBER (data not shown).

Immunohistochemistry for LMP-1 was also performed in periapical granulomas and healthy gingival tissues. All of the EBER-positive periapical granulomas that were confirmed by ISH showed positive staining for LMP-1 (Fig. 5A, B). LMP-1 was expressed by B lymphocytes and plasma cells. In addition, EBER-expressing cells were localized to the same areas as LMP-1-expressing cells, based on serial tissue sections (Fig. 5C, D). A negative control using normal mouse IgG antibody did not exhibit LMP-1 expression (Fig. 5E, F). Healthy gingival tissues showed negative expression of LMP-1 (data not shown).

Quantitative Detection of *P. endodontalis* using Real-time PCR

P. endodontalis DNA in periapical granulomas was detected using real-time PCR. In all, 32 of the 50 periapical granulomas (64.0%) showed *P. endodontalis*. The relationship between the presence of EBV and *P. endodontalis* was not observed in each periapical granulomas (Fig. 6). In healthy gingival tissues, EBV DNA was never detected; however, *P. endodontalis* was detected in 5 of 10 samples (50.0%) (data not shown).

Quantitative Analysis of *n*-Butyric Acid in *P. endodontalis* Culture Supernatants

Culture supernatants of *P. endodontalis* were collected after 5 days of culture (n = 5) and the concentration of *n*-butyric acid was measured using ion-exclusion HPLC. The concentration of *n*-butyric acid produced from *P. endodontalis* was 23.38 ± 3.67 mM (data not shown).

Detection of BZLF-1 mRNA Expression using Real-time PCR

Daudi cell line was treated with *n*-butyric acid (1.0 mM) in 12-well culture plates for 48 h. Cells were harvested and mRNA was then extracted, reverse-transcribed and amplified by real-time PCR for BZLF-1. BZLF-1 mRNA expression in the treated cell lines was significantly higher than untreated (Fig. 7A).

Daudi cell line was also treated with the supernatants of *P. endodontalis* (1.2 mM) in 12-well culture plates for 3, 6, 12, and 24 h. After the indicated time, the cells were harvested and BZLF-1 mRNA expression was detected by real-time PCR. The expression level of BZLF-1 increased in a time-dependent manner (Fig. 7B).

Discussion

In this study, EBV was detected in 76.0% (38 of 50 samples) of periapical granulomas by real-time PCR. The presence of EBV in periapical lesions has been examined by immunohistochemistry for EBNA or PCR (12-14), and the EBV detection rate varied from 54.6-85.7%. Possible reasons for the variation among previous studies include differences in EBV detection methods, disease status, or regional features of EBV infection. The EBV detection rates were relatively high compared with those in published data. This study determined the EBV DNA copy numbers in periapical granulomas, which have not yet been reported. The median EBV DNA copy number in periapical granulomas was 6,634.00 / μ g total DNA; in contrast, EBV was not detected in healthy tissues. Therefore, EBV may be important in the initiation of periapical inflammation or may prolong apical inflammation as a result of increasing tissue damage.

EBV causes systemic diseases such as infectious mononucleosis. On the other hand, EBV induces immune dysregulation by inhibiting the replication of stimulated peripheral blood mononuclear leukocytes (23). In addition, it up-regulates proinflammatory cytokines such as TNF- α , IL-1 β , IL-6, IL-8, and IL-10 (24-26). IL-10 is produced by T helper type-2 (Th2) lymphocytes, monocytes, macrophages, and B lymphocytes, and it inhibits the production of cytokines such as IL-2 and interferon- γ by Th1 lymphocytes (27). Th1 cytokines are important in controlling viral infections, and a shift in the cytokine profile toward Th2 could be favorable for virus-induced inflamed lesions. Thus, EBV infection may play a role in not only systemic but also local, inflammatory disease. In this study, EBV DNA was absent from healthy gingival tissues, suggesting that elevated levels of EBV in periapical granulomas contribute to immune reactions in periapical lesions, including tissue destruction and bone resorption. Those data also indicate that local, inflamed lesions could be an EBV reservoir for systemic infections, supplying the virus through the blood via microvessels in granulomatous tissues.

Although the presence of EBV in periapical lesions has been examined (12-14), it has not been confirmed. In this study, EBER was detected in B lymphocytes and plasma cells in periapical granulomas using ISH, whereas healthy gingival tissues did not show EBER expression. Those data suggest that in periapical granulomas, these cells were

infected with EBV because the presence of EBER is considered a reliable marker for the existence of latent EBV in cells (15). EBER was also found to be expressed in the nucleus and cytoplasm of cells. EBER expression has been detected in the nuclei of B lymphocytes in gastric carcinoma or tonsillar tissues from patients with tonsillitis by ISH (28, 29). However, Schwemmler *et al.* (30) demonstrated that EBER was located in both the cytoplasm and nucleus of cells using ISH and confocal laser microscopy. EBER was found to be secreted in a complex with La protein (31). Thus, EBER forms complexes with cytoplasmic proteins and could localize to both the nucleus and the cytoplasm.

Immunohistochemistry using serial tissue sections demonstrated the presence of LMP-1-expressing cells in the same regions as EBER-expressing cells, in accordance with EBER ISH results. On the other hand, the EBER expression rate in periapical granulomas was 66.7% for EBV-positive specimens confirmed by real-time PCR. The reason for the lower detection rate by ISH could be that the sensitivity of ISH is lower than that of real-time PCR.

The functional role of EBER in periapical granulomas is unclear; however, it has been demonstrated that EBER induces transcription of cytokines, including IL-10, insulin-like growth factor-1, and IL-9 (32-34). It also contributes to the pathogenesis of EBV infection through modulation of innate immune signals (31). Therefore, EBER-induced

activation of innate immunity could account for immunopathologic diseases caused by EBV infection and could influence the pathogenesis of EBV-induced diseases. In addition, EBV-associated IL-10 expression has been detected in periapical lesions (35). Thus, EBER could be associated with the pathogenesis of periapical granulomas by way of subsequent immune activation.

Latent EBV is reactivated by the association with bacterial *n*-butyric acid, and *P. endodontalis* was utilized in this study. The existence of *P. endodontalis* and EBV in periapical granulomas was first determined by quantitative real-time PCR. The percentages of *P. endodontalis* and EBV detection were 64.0% and 76.0%, respectively, and the detection rate was similar to previous findings (36, 37). However, the relationship between EBV and *P. endodontalis* was not observed in each periapical granulomas. It could be that *P. endodontalis* was decreased by the calcium hydroxide dressing during root canal treatments for long-term periods before endodontic surgery. In healthy gingival tissues (n = 10), EBV DNA was not detected; however, *P. endodontalis* was found in 5 patients. The reason for the detection of *P. endodontalis* in healthy gingival tissues could be that the PCR technique is highly sensitive in detecting gene expression. H-E stains of healthy gingival tissues showed considerably fewer inflammatory cells compared with periapical granulomas, suggesting that

P. endodontalis does not mediate inflammation in healthy gingival tissues.

To determine the potential of *P. endodontalis* to reactivate latent EBV, the concentration of *n*-butyric acid in the culture supernatant of *P. endodontalis* was determined using ion-exclusion HPLC. *P. endodontalis* produced *n*-butyric acid, and it was hypothesized that *P. endodontalis* could reactivate latent EBV in periapical granulomas.

It was still unclear whether *n*-butyric acid from *P. endodontalis* might reactivate latent EBV. Therefore, the expression of BZLF-1, known as a potent marker of the EBV reactivation, was examined using Daudi cell line. Daudi cell line was established from peripheral blood obtained from Burkitt's lymphoma patients and is well known as a EBV-positive B-lymphoblastoid cell line. In this study, Daudi cell line was treated with commercially available *n*-butyric acid or the supernatant of *P. endodontalis*, and BZLF-1 mRNA expression was examined using real-time PCR. BZLF1 mRNA expression of Daudi cell line treated with *n*-butyric acid was clearly higher than untreated. In addition, the expression level was up-regulated in a time-dependent manner when Daudi cell line was treated with the supernatant of *P. endodontalis*. The data suggested the possibility that latent EBV could be reactivated by *n*-butyric acid produced from *P. endodontalis*.

Reactivated EBV can enhance the expression of inflammatory cytokines by

macrophages and induce chronic inflammation (38). It has also been hypothesized that cytokine expression in periapical lesions could be correlated with the presence of EBV (35). EBV stays in latency if BZLF-1 mRNA is not expressed, suggesting that inflammation could not be initiated or exacerbated if viral replication was inhibited. Thus, a local drug delivery system using therapeutic agents to prevent BZLF-1 expression could be useful as a novel endodontic treatment. Interestingly, the expression of BZLF-1 mRNA was inhibited by the application of L-arginine (39), suggesting that the lytic and latent cycles of EBV might be controlled precisely with nitric oxide in inflamed areas. Further animal studies might be beneficial to resolve these hypotheses.

Conclusions

In this study, the following results about the evidence of EBV infection in periapical granulomas and suggests a mechanism for EBV reactivation were obtained.

1. EBV and *P. endodontalis* were detected using real-time PCR in periapical granulomas.
2. EBER, known as a reliable marker of EBV infection, and LMP-1 were detected at B lymphocytes and plasma cells in periapical granulomas.
3. Latent EBV in Daudi cell line was reactivated by *n*-butyric acid produced from

P. endodontalis.

On the basis of these observations, it is concluded that latent EBV infected in periapical granulomas could be reactivated by *P. endodontalis* and EBV reactivation might exacerbate periapical pathosis.

Acknowledgements

I would like to thank Prof. Bunnai Ogiso and Associate Prof. Osamu Takeichi of Department of Endodontics, Nihon University School of Dentistry, and Prof. Kuniyasu Ochiai and Associate Prof. Kenichi Imai of Department of Microbiology, Nihon University School of Dentistry for their valuable scientific comments, technical advice and support. This study was supported by grants from Grant-in-Aid for Scientific Research (C) for 2012-2015 (Osamu Takeichi) and from Nihon University Graduate School Dental Research Center for 2013 and 2014 (Kosuke Makino).

References

1. Siqueira JF Jr, Rôças IN (2009) Distinctive features of the microbiota associated with different forms of apical periodontitis. *J Oral Microbiol* 1, 1-12.
2. Nair PN (2004) Pathogenesis of apical periodontitis and the causes of endodontic failures. *Crit Rev Oral Biol Med* 15, 348-381.
3. Siqueira JF Jr, Rôças IN (2009) Diversity of endodontic microbiota revisited. *J Dent Res* 88, 969-981.
4. Windley W 3rd, Teixeira F, Levin L, Sigurdsson A, Trope M (2005) Disinfection of immature teeth with a triple antibiotic paste. *J Endod* 31, 439-443.
5. Jungermann GB, Burns K, Nandakumar R, Tolba M, Venezia RA, Fouad AF (2011) Antibiotic resistance in primary and persistent endodontic infections. *J Endod* 37, 1337-1344.
6. Küppers R (2003) B cells under influence: transformation of B cells by Epstein-Barr virus. *Nat Rev Immunol* 3, 801-812.
7. Morris MA, Dawson CW, Wei W, O'Neil JD, Stewart SE, Jia J et al. (2008) Epstein-Barr virus encoded LMP1 induces a hyperproliferative and inflammatory gene expression programme in cultured keratinocytes. *J Gen Virol* 89, 2806-2820.
8. Murakami M, Hashida Y, Imajoh M, Maeda A, Kamioka M, Senda Y et al. (2014) PCR array analysis of gene expression profiles in chronic active Epstein-Barr virus infection. *Microbes Infect* 16, 581-586.
9. Rahal EA, Hajjar H, Rajeh M, Yamout B, Abdelnoor AM (2015) Epstein-Barr virus and human herpes virus 6 type A DNA enhance IL-17 production in mice. *Viral Immunol* 28, 297-302.
10. Sawada S, Takei M, Inomata H, Nozaki T, Shiraiwa H (2007) What is after cytokine-blocking therapy, a novel therapeutic target—synovial Epstein-Barr virus for rheumatoid arthritis. *Autoimmun Rev* 6, 126-130.
11. Kivity S, Arango MT, Ehrenfeld M, Tehori O, Shoenfeld Y, Anaya JM et al. (2014) Infection and autoimmunity in Sjögren's syndrome: a clinical study and comprehensive review. *J Autoimmun* 51, 17-22.
12. Sabeti M, Simon JH, Slots J (2003) Cytomegalovirus and Epstein-Barr virus are associated with symptomatic periapical pathosis. *Oral Microbiol Immunol* 18, 327-328.
13. Chen V, Chen Y, Li H, Kent K, Baumgartner JC, Machida CA (2009) Herpesviruses in abscesses and cellulitis of endodontic origin. *J Endod* 35, 182-188.
14. Guilherme BP, Ferreira DC, Rôças IN, Provenzano JC, Santos KR, Siqueira JF Jr

- (2011) Herpesvirus carriage in saliva and posttreatment apical periodontitis: searching for association. *Oral Surg Oral Med Oral Pathol Oral Radiol Endod* 112, 678-683.
15. Chang KL, Chen YY, Shibata D, Weiss LM (1992) Description of an in situ hybridization methodology for detection of Epstein-Barr virus RNA in paraffin-embedded tissues, with a survey of normal and neoplastic tissues. *Diagn Mol Pathol* 1, 246-255.
 16. Countryman J, Miller G (1985) Activation of expression of latent Epstein-Barr herpesvirus after gene transfer with a small cloned subfragment of heterogeneous viral DNA. *Proc Natl Acad Sci USA* 82, 4085-4089.
 17. Hsu CH, Hergenahn M, Chuang SE, Yeh PY, Wu TC, Gao M et al. (2002) Induction of Epstein-Barr virus (EBV) reactivation in Raji cells by doxorubicin and cisplatin. *Anticancer Res* 22, 4065-4071.
 18. Gomes BP, Endo MS, Martinho FC (2012) Comparison of Endotoxin Levels Found in Primary and Secondary Endodontic Infections. *J Endod* 38, 1082-1086.
 19. Mirucki CS, Abedi M, Jiang J, Zhu Q, Wang YH, Safavi KE et al. (2014) Biologic activity of *Porphyromonas endodontalis* complex lipids. *J Endod* 40, 1342-1348.
 20. Murakami Y, Hanazawa S, Tanaka S, Iwahashi H, Yamamoto Y, Fujisawa S (2001) A possible mechanism of maxillofacial abscess formation: involvement of *Porphyromonas endodontalis* lipopolysaccharide via the expression of inflammatory cytokines. *Oral Microbiol Immunol* 16, 321-325.
 21. Tang Y, Sun F, Li X, Zhou Y, Yin S, Zhou X (2011) *Porphyromonas endodontalis* lipopolysaccharides induce RANKL by mouse osteoblast in a way different from that of *Escherichia coli* lipopolysaccharide. *J Endod* 37, 1653-1658.
 22. Tsukahara T, Matsukawa N, Tomonaga S, Inoue R, Ushida K, Ochiai K (2014) High-sensitivity detection of short-chain fatty acids in porcine ileal, cecal, portal and abdominal blood by gas chromatography-mass spectrometry. *Anim Sci J* 85, 494-498.
 23. Glaser R, Litsky ML, Padgett DA, Baiocchi RA, Yang EV, Chen M et al. (2006) EBV-encoded dUTPase induces immune dysregulation: Implications for the pathophysiology of EBV-associated disease. *Virology* 346, 205-218.
 24. Chong JM, Sakuma K, Sudo M, Osawa T, Ohara E, Uozaki H et al. (2002) Interleukin-1 β expression in human gastric carcinoma with Epstein-Barr virus infection. *J Virol* 76, 6825-6831.
 25. Sin SH, Dittmer DP (2011) Cytokine homologs of human gammaherpesviruses. *J*

- Interferon Cytokine Res 32, 53-59.
26. Nakai H, Kawamura Y, Sugata K, Sugiyama H, Enomoto Y, Asano Y et al. (2012) Host factors associated with the kinetics of Epstein-Barr virus DNA load in patients with primary Epstein-Barr virus infection. *Microbiol Immunol* 56, 93-98.
 27. Fiorentino DF, Zlotnik A, Mosmann TR, Howard M, O'Garra A (1991) IL-10 inhibits cytokine production by activated macrophages. *J Immunol* 147, 3815-3822.
 28. Szkaradkiewicz A, Majewski W, Wal M, Czyzak M, Majewski P, Bierła J et al. (2006) Epstein-Barr virus (EBV) infection and p53 protein expression in gastric carcinoma. *Virus Res* 118, 115-119.
 29. Endo LH, Ferreira D, Montenegro MC, Pinto GA, Altemani A, Bortoleto AE Jr et al. (2001) Detection of Epstein-Barr virus in tonsillar tissue of children and the relationship with recurrent tonsillitis. *Int J Pediatr Otorhinolaryngol* 58, 9-15.
 30. Schwemmler M, Clemens MJ, Hulse K, Pfeifer K, Tröster H, Müller WE et al. (1992) Localization of Epstein-Barr virus-encoded RNAs EBER-1 and EBER-2 in interphase and mitotic Burkitt lymphoma cells. *Proc Natl Acad Sci USA* 89, 10292-10296.
 31. Iwakiri D, Zhou L, Samanta M, Matsumoto M, Ebihara T, Seya T et al. (2009) Epstein-Barr virus (EBV)-encoded small RNA is released from EBV-infected cells and activates signaling from Toll-like receptor 3. *J Exp Med* 206, 2091-2099.
 32. Iwakiri D, Sheen TS, Chen JY, Huang DP, Takada K (2005) Epstein-Barr virus-encoded small RNA induces insulin-like growth factor 1 and supports growth of nasopharyngeal carcinoma-derived cell lines. *Oncogene* 24, 1767-1773.
 33. Samanta M, Iwakiri D, Takada K (2008) Epstein-Barr virus-encoded small RNA induces IL-10 through RIG-I-mediated IRF-3 signaling. *Oncogene* 27, 4150-4160.
 34. Yang L, Aozasa K, Oshimi K, Takada K (2004) Epstein-Barr virus (EBV)-encoded RNA promotes growth of EBV-infected T cells through interleukin-9 induction. *Cancer Res* 64, 5332-5337.
 35. Sabeti M, Kermani V, Sabeti S, Simon JH (2012) Significance of human cytomegalovirus and Epstein-Barr virus in inducing cytokine expression in periapical lesions. *J Endod* 38, 47-50.
 36. Slots J, Saygun I, Sabeti M, Kubar A (2006) Epstein-Barr virus in oral diseases. *J Periodontal Res* 41, 235-244.
 37. Gomes BP, Pinheiro ET, Jacinto RC, Zaia AA, Ferraz CC, Souza-Filho EJ (2008) Microbial analysis of canals of root-filled teeth with periapical lesions using polymerase chain reaction. *J Endod* 34, 537-540.
 38. Waldman WJ, Williams MV Jr, Lemeshow S, Binkley P, Guttridge D,

- Kiecolt-Glaser JK et al. (2008) Epstein-Barr virus-encoded dUTPase enhances proinflammatory cytokine production by macrophages in contact with endothelial cells: evidence for depression-induced atherosclerotic risk. *Brain Behav Immun* 22, 215-223.
39. Agawa H, Ikuta K, Minamiyama Y, Inoue M, Sairenji T (2002) Down-regulation of spontaneous Epstein-Barr virus reactivation in the P3HR-1 cell line by L-arginine. *Virology* 304, 114-124.

Table and Figures

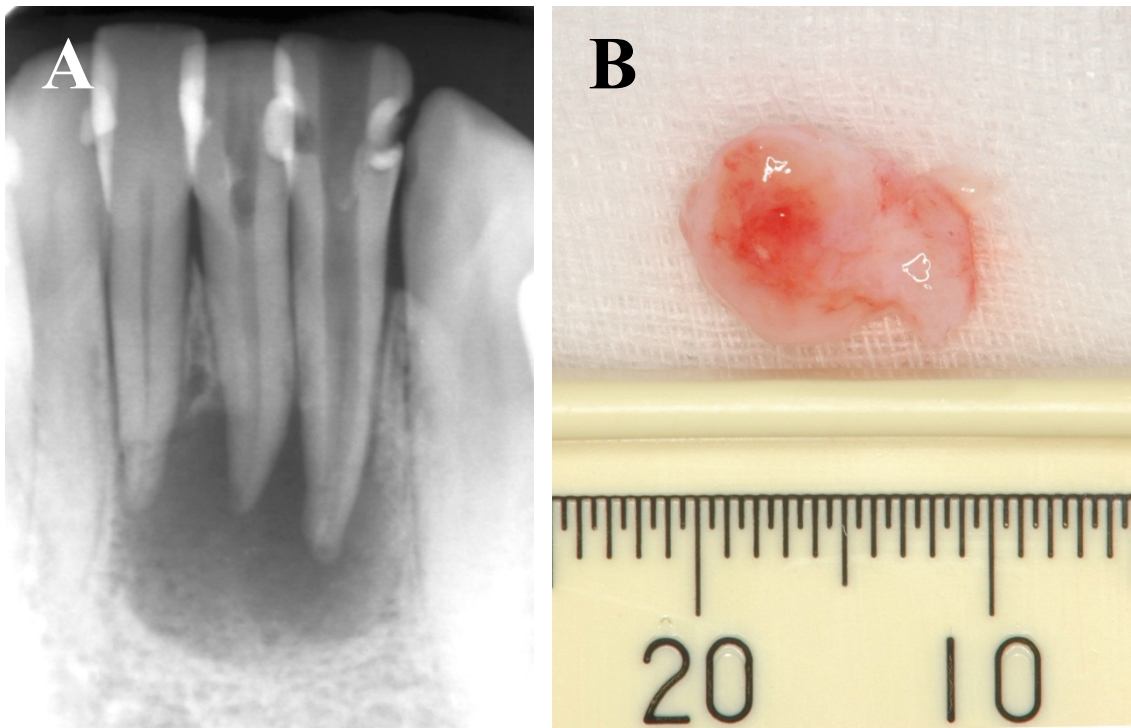


Figure 1

Specimens used in this study. (A) X-ray observation of periapical lesions caused at lower incisal teeth. Radiolucency around the apex showed alveolar bone resorption. (B) Periapical lesion surgically removed from a patient showing at (A).

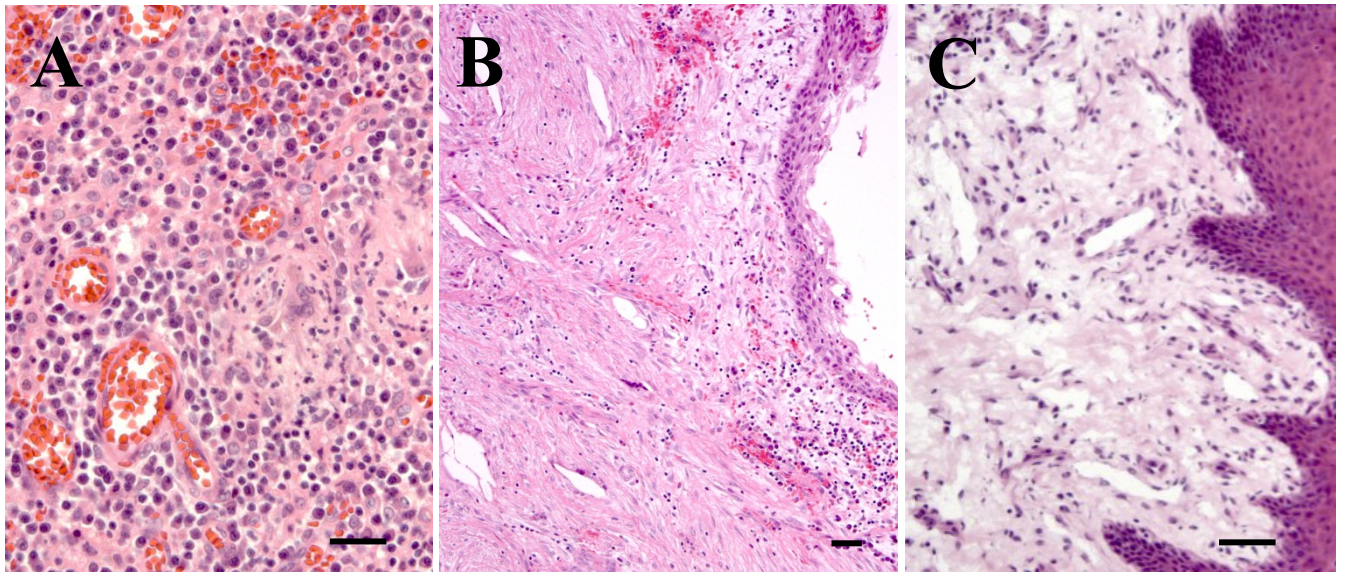
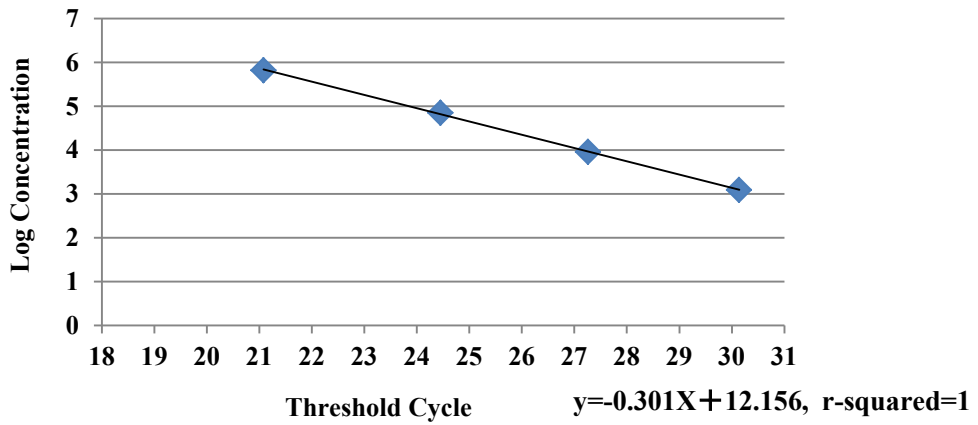
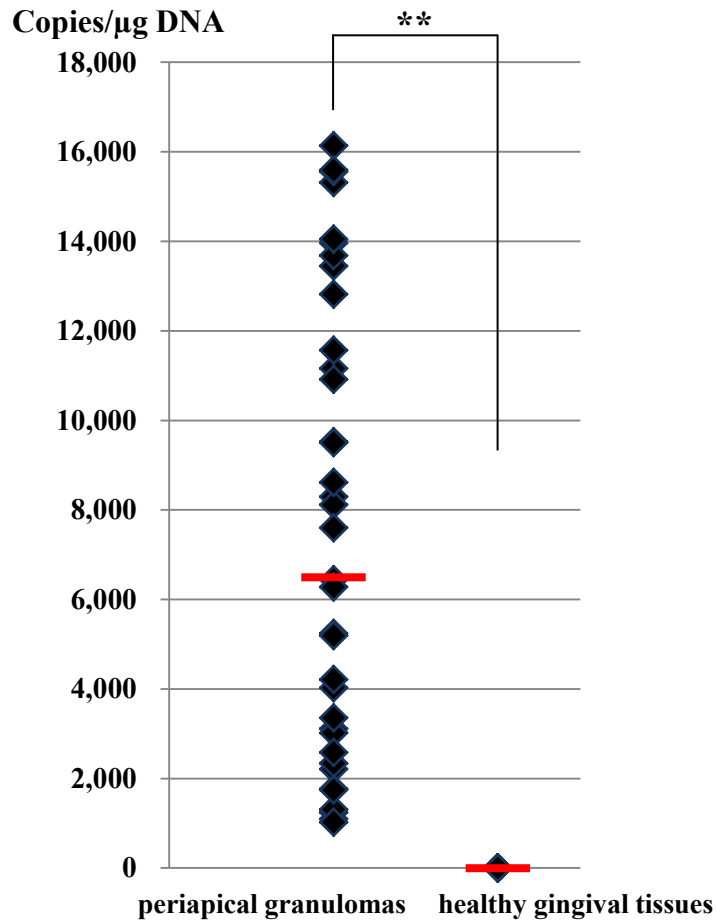


Figure 2

Histological evaluations of the specimens. Paraffin sections (n = 63) were stained using hematoxylin and eosin. Scale bar = 100 μ m. (A) Periapical granulomas (n = 50) showing a large number of inflammatory cells and microvessels. (B) Radicular cyst (n = 13) showing epithelial cell layer and cholesterol clefts. (C) Healthy gingival tissues (n = 10) showing epithelial cell layer and lower cell number of infiltrating cells in comparison with periapical granulomas.

A**B****Figure 3**

Quantitative real time PCR analysis. (A) Standard curve to determine the copies of EBV DNA in specimens. EBV DNA (approximately 1×10^6 copies/ μl) was diluted in ten-fold serially. Each diluted DNA was amplified using real-time PCR simultaneously at the time of amplification for DNA extracted from periapical granulomas and healthy gingivae. (B) Detection of EBV DNA in periapical granulomas and healthy gingivae. The copy of EBV DNA in each specimen was calculated using the standard curve. The median of EBV DNA copies in periapical granulomas was approximately 6,634.00 per 1 μg of total DNA, as shown by a horizontal bar. ** showed statistical difference using Mann-Whitney U test ($p = 0.0001$).

Table 1 Detection of EBV DNA using quantitative real-time PCR.

	periapical granulomas (n = 50)	healthy gingival tissues (n = 10)	<i>P</i>-value
presence	38 (76.0%)	0 (0.0%)	0.0001**
absence	12 (24.0%)	10 (100.0%)	

Periapical granulomas and healthy gingival tissues were analyzed to detect EBV DNA by quantitative real-time PCR. EBV DNA was highly detected from periapical granulomas in comparison with healthy gingival tissues.

** Mann-Whitney *U*-test.

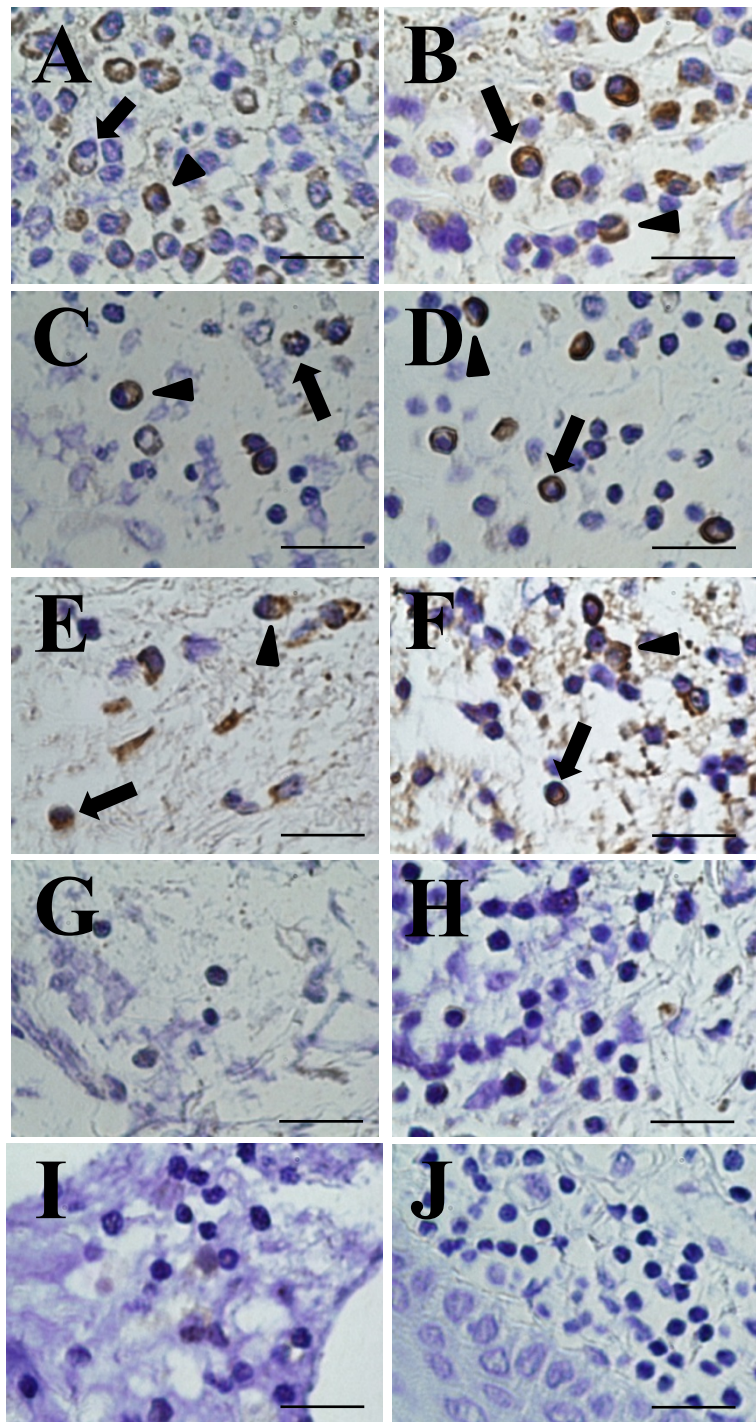


Figure 4

Detection of EBER using *in situ* hybridization. (A-F) *In situ* detection of EBER-expressing cells in periapical granulomas (6 out of 9) was shown in the cytoplasm and nuclei of B lymphocytes (arrows) and plasma cells (arrow heads). (G-I) Three periapical granulomas showed EBER-negative expression. (J) Healthy gingival tissues never showed positive expression. Scale bar = 50 μm .

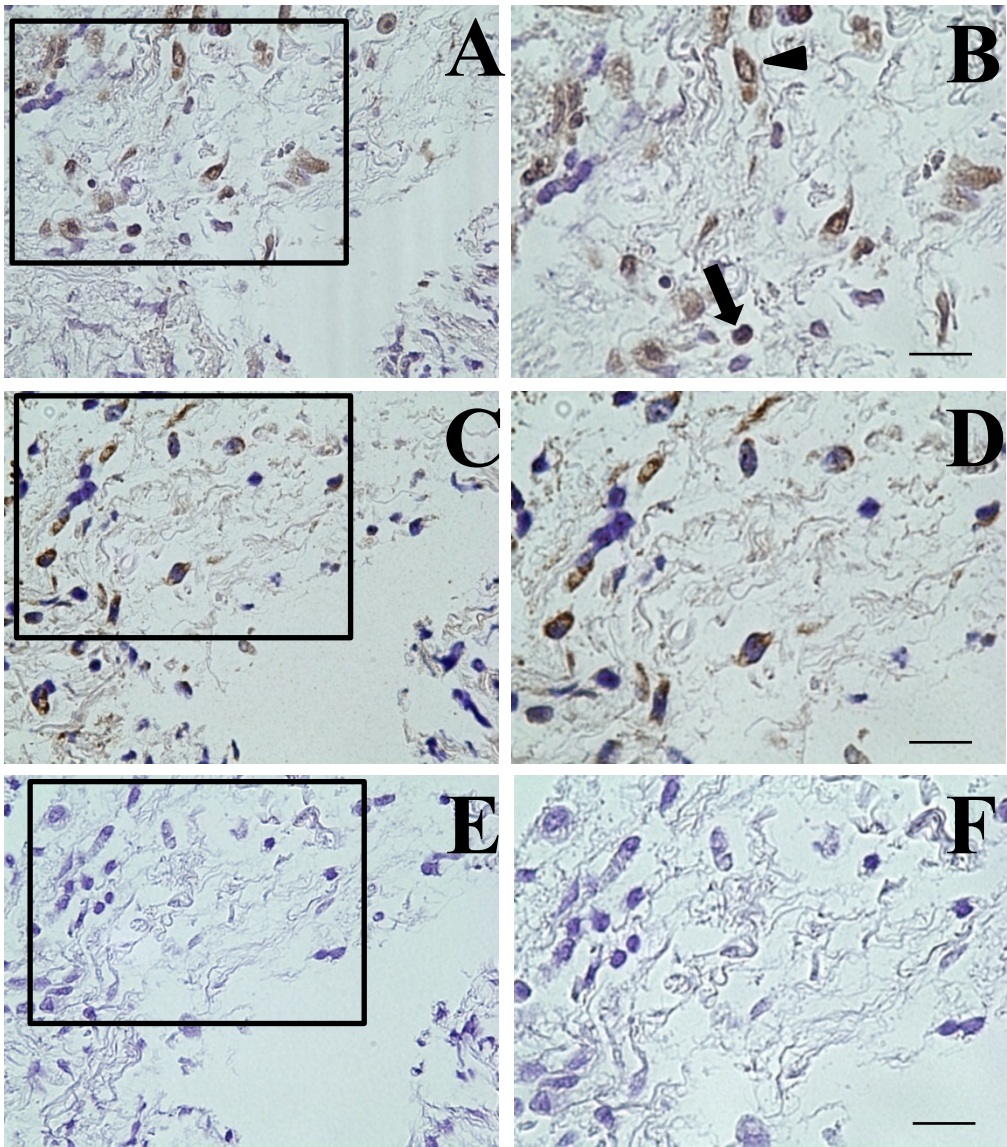


Figure 5

LMP-1 immunohistochemistry using serial sections of periapical granulomas. Framed boxes in left panels (A, C, E) were magnified to right panels (B, D, F, respectively). (A, B) LMP-1 immunohistochemistry showed positive staining in B lymphocytes (arrows) and plasma cells (arrow heads). (C, D) EBER-expressing cells were present at the same area of LMP-1-expressing cells. (E, F) A negative control using normal mouse IgG antibody did not exhibit LMP-1 expression. Scale bar = 50 μ m.

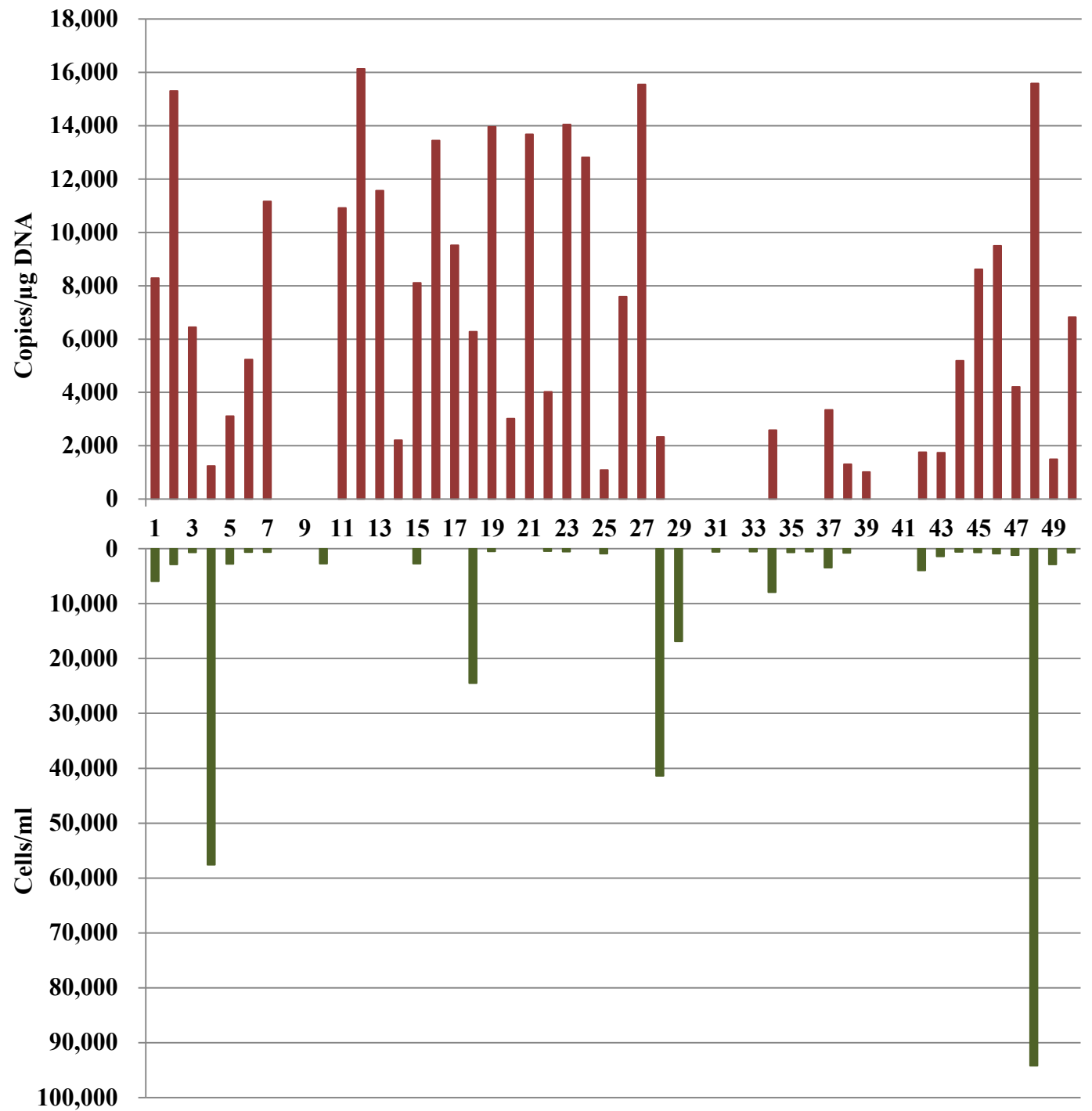
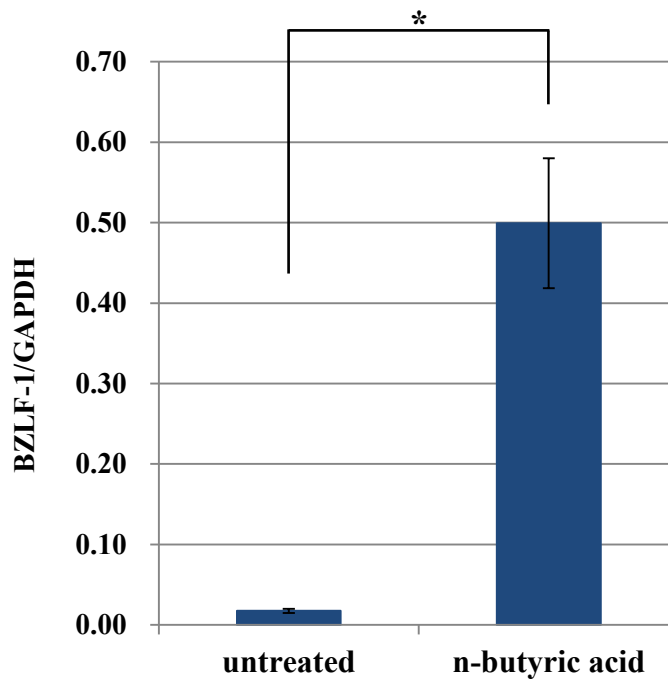
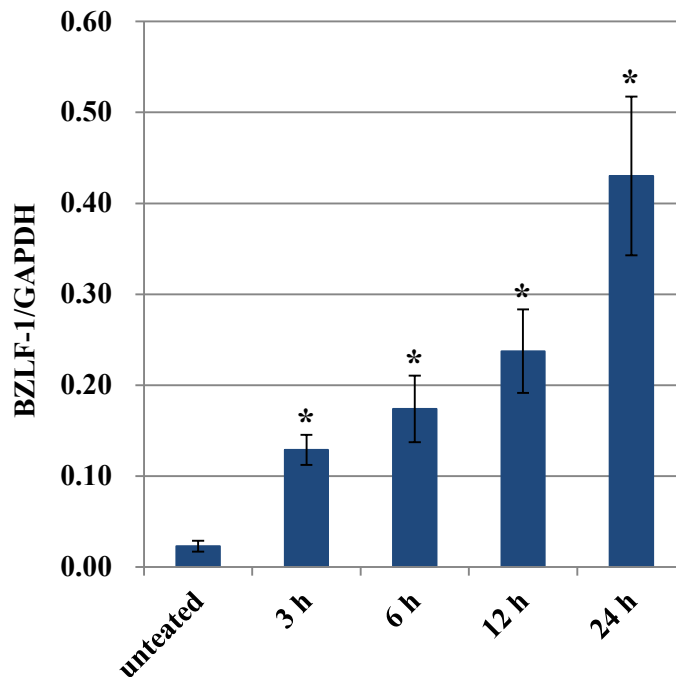


Figure 6

Quantitative real-time PCR analysis to detect EBV and *P. endodontalis*. The detection of EBV (upper) and *P. endodontalis* (lower) was shown. The percentage of the detection rate was 76.0% and 64.0% for EBV and *P. endodontalis*, respectively.

A**B****Figure 7**

Expression of BZLF-1 mRNA in Daudi cell line using real time PCR. (A) BZLF-1 mRNA expression of untreated and treated with commercially available n-butyric acid (1.0 mM). Statistical analysis was performed using Student's *t*-test ($*p < 0.05$). (B) BZLF-1 mRNA expression in Daudi cell line treated with the supernatants of *P. endodontalis* (1.2 mM) for 3, 6, 12, and 24 h. The difference was statistically analyzed by Dunnett's test ($*p < 0.05$, vs untreated)